# Prediction of Absolute Rate Constants for the Reactions of $NH_2$ with Alkanes from ab Initio G2M/TST Calculations

**A. M. Mebel[†,‡] and M. C. Lin*[,§]**

*Institute of Atomic and Molecular Sciences, Academia Sinica, P.O. Box 23-166, Taipei 106, Taiwan, Department of Chemistry, Tamkang University, Tamsui 25137, Taiwan, and Department of Chemistry, Emory University, Atlanta, Georgia 30322*

*Received: November 20, 1998; In Final Form: February 3, 1999*

Systematic ab initio calculations of potential energy surfaces for the reactions of $NH_2$ with various alkanes ($CH_4$, $C_2H_6$, $C_3H_8$, and *i*-$C_4H_{10}$) which involve abstraction of a hydrogen atom from primary, secondary, and tertiary C−H bonds have been performed using the G2M method. The calculated activation barrier for the $NH_2 + CH_4$ reaction, 15.2 kcal/mol, is higher than those for the H-abstraction from a primary C−H bond in $C_2H_6$, $C_3H_8$, and *i*-$C_4H_{10}$, 11−12 kcal/mol. The barrier height decreases to 8.4 and 8.3 kcal/mol for the abstraction from a secondary C−H bond in $C_3H_8$ and a tertiary C−H bond in *i*-$C_4H_{10}$, respectively, in line with the weakening strength of the C−H bond and the increase of the reaction exothermicity. The G2M energies and the molecular and transition-state parameters are used to compute thermal reaction rate constants within the transition-state theory formalism with tunneling corrections. A good agreement of the theoretical rate constants with the experimental is found if the computed barriers are adjusted by 0.5−2 kcal/mol, which is within the accuracy of the G2M method. The H-abstraction from the tertiary C−H bond is shown to be faster than the other considered reactions at $T \leq 2000$ K, while the secondary H-abstraction is the second fastest reaction at $T \leq 1600$ K. The rate of the primary H-abstraction decreases with the increase of the alkane size, from ethane to propane and to isobutane. The calculated rate constants for the H-abstraction by $NH_2$ from primary, secondary, and tertiary C−H bonds can serve as models for the reactions of the amino radical with various saturated hydrocarbons.

## Introduction

Reactions of the amino radical, $NH_2$, are relevant to planetary atmospheric chemistry, particularly those of Jupiter and Titan[1] as well as to the $NH_3$ de$NO_x$[2] and HNCO RAPRE$NO_x$ (rapid reduction of $NO_x$)[3] processes and have recently attracted much attention. The reactions of $NH_2$ with saturated hydrocarbons proceed by direct abstraction of the hydrogen atom from RH giving $NH_3$ and alkyl radicals R. These reactions are relatively well studied experimentally, and their rate constants are reported for a broad temperature range. For instance, Demissy and Lesclaux[4] measured the reactions with a series of alkanes including methane, ethane, propane, isobutane, and *n*-butane at temperatures between 300 and 520 K. They performed their measurements by flash photolysis using laser-resonance absorption for the detection of $NH_2$. Hack et al.[5−7] used an isothermal flow system to study the reactions of $NH_2$ with $CH_4$, $C_2H_6$, $C_3H_8$, isobutane, and cyclohexane. [$NH_2$](t)-profiles were measured at temperatures from 400 to 1080 K with the laser-induced fluorescence (LIF) technique. Hennig and Wagner[8] used the shock tube method to measure reactions of $NH_2$ with methane, ethane, and propane at temperatures between 1500 and 2100 K. The experimental rate constants for the reactions of $NH_2$ with alkanes are collected in Table 1. Hennig and Wagner suggested three-parameter expressions for the $NH_2 + CH_4$, $NH_2 + C_2H_6$, and $NH_2 + C_3H_8$ reactions that fit the rate constants for different temperature ranges.

On the other hand, theoretical calculations on the reactions of $NH_2$ with saturated hydrocarbons are scarce and limited only to the reaction with methane. Leroy, Sana, and co-workers[9,10] studied the $NH_2 + CH_4 \rightarrow NH_3 + CH_3$ reaction at the CI//UHF/6-31G level. Recently, Basch and Hoz[11] carried out more accurate UMP2, CCSD(T)//UMP2, and B3LYP calculations with the 6-311++G(2d,p) basis set. We have studied this reaction using the G2M approach, computed absolute rate constants employing the transition-state theory (TST), and investigated the kinetic isotope effects.[12]

In the present paper, we report systematic G2M calculations of potential energy surfaces for the reactions of $NH_2$ with various alkanes that include abstraction of the hydrogen atom from primary, secondary, and tertiary C−H bond:

$$NH_2 + CH_4 \rightarrow NH_3 + CH_3 \quad (1)$$

$$NH_2 + C_2H_6 \rightarrow NH_3 + C_2H_5 \quad (2)$$

$$NH_2 + C_3H_8 \rightarrow NH_3 + i\text{-}C_3H_7 \quad (3a)$$

$$NH_2 + C_3H_8 \rightarrow NH_3 + n\text{-}C_3H_7 \quad (3b)$$

$$NH_2 + i\text{-}C_4H_{10} \rightarrow NH_3 + t\text{-}C_4H_9 \quad (4a)$$

$$NH_2 + i\text{-}C_4H_{10} \rightarrow NH_3 + i\text{-}C_4H_9 \quad (4b)$$

The results for reaction 1 published earlier[12] are given for comparison. The ab initio data are used to compute reaction thermal rate constants that are compared with experimental measurements.

[†] Institute of Atomic and Molecular Sciences, Academia Sinica.
[‡] Department of Chemistry, Tamkang University.
[§] Department of Chemistry, Emory University.

10.1021/jp9844922 CCC: $18.00 
Published on Web 03/12/1999

**TABLE 1: Heats of Reactions (kcal/mol), Activation Barriers (kcal/mol) Calculated at the G2M(rcc,MP2) Level, and Rate Constants for the Reactions of $NH_2$ with Saturated Hydrocarbons**

| reaction | $\Delta E^a$ | $\Delta H_{exp}$ (298)[b] | $\Delta E^{\#}$ clas[c] | $\Delta E^{\#}$ qm[d] | $\Delta E^{\#}$ adj[e] | theoretical rate constant[f] ($cm^3$/molecule·s) | experimental rate constant ($cm^3$/molecule·s) |
|---|---|---|---|---|---|---|---|
| $NH_2 + CH_4 \rightarrow NH_3 + CH_3$ (1) | −2.3 | −2.6 | 15.0 | 14.9 | 14.4 | $(4.49 \times 10^{-23})T^{3.60}e^{-4775/T}$<br>$(5.12 \times 10^{-23})T^{3.59}e^{-4545/T}$(adj) | 300−520 K:[g] $(8.30 \times 10^{-13})e^{-10500/RT}$<br>740−1030 K:[h] $(9.63 \times 10^{-12})e^{-13169/RT}$<br>1740−2140 K:[i] $(1.99 \times 10^{-11})e^{-15153/RT}$<br>300−2100 K:[i] $(1.18 \times 10^{-18})T^{2.0}e^{-4690/T}$ |
| $NH_2 + C_2H_6 \rightarrow NH_3 + C_2H_5$ (2) | −5.7 | −6.4 | 12.8 | 12.2 | 10.2 | $(4.05 \times 10^{-23})T^{3.54}e^{-3719/T}$<br>$(7.54 \times 10^{-23})T^{3.46}e^{-2820/T}$(adj) | 300−520 K:[g] $(6.14 \times 10^{-13})e^{-7150/RT}$<br>598−973 K:[j] $(1.61 \times 10^{-11})e^{-10612/RT}$<br>1500−1900 K:[i] $(1.61 \times 10^{-11})e^{-11472/RT}$<br>300−2000 K:[i] $(5.09 \times 10^{-18})T^{1.8}e^{-3185/T}$ |
| $NH_2 + C_3H_8 \rightarrow NH_3 + i\text{-}C_3H_7$ (3a) | −8.2 | −8.8 | 9.3 | 8.4 | 7.9 | $(1.71 \times 10^{-22})T^{3.30}e^{-2447/T}$<br>$(1.93 \times 10^{-22})T^{3.29}e^{-2218/T}$(adj) | |
| $NH_2 + C_3H_8 \rightarrow NH_3 + n\text{-}C_3H_7$ (3b) | −5.0 | −7.0 | 11.7 | 11.1 | 10.6 | $(5.75 \times 10^{-23})T^{3.51}e^{-3401/T}$<br>$(6.71 \times 10^{-23})T^{3.49}e^{-3175/T}$(adj) | |
| $NH_2 + C_3H_8 \rightarrow NH_3 + C_3H_7$ (3) | | | | | | $(2.98 \times 10^{-23})T^{3.62}e^{-2474/T}$<br>$(3.49 \times 10^{-23})T^{3.60}e^{-2249/T}$(adj) | 300−520 K:[g] $(7.47 \times 10^{-13})e^{-6150/RT}$<br>550−1073 K:[j] $(1.41 \times 10^{-11})e^{-9393/RT}$<br>1500−1900 K:[i] $(2.82 \times 10^{-11})e^{-10660/RT}$<br>300−2000 K:[i] $(2.87 \times 10^{-18})T^{2.0}e^{-3210/T} + (1.66 \times 10^{-13})e^{-1600/T}$ |
| $NH_2 + i\text{-}C_4H_{10} \rightarrow NH_3 + t\text{-}C_4H_9$ (4a) | −9.8 | −11.0 | 8.3 | 8.3 | 7.3 | $(3.61 \times 10^{-22})T^{3.20}e^{-2366/T}$<br>$(5.20 \times 10^{-22})T^{3.16}e^{-1925/T}$(adj) | |
| $NH_2 + i\text{-}C_4H_{10} \rightarrow NH_3 + i\text{-}C_4H_9$ (4b) | −5.0 | −7.4 | 12.0 | 12.4 | 11.4 | $(1.15 \times 10^{-23})T^{3.65}e^{-3780/T}$<br>$(1.69 \times 10^{-23})T^{3.61}e^{-3342/T}$(adj) | |
| $NH_2 + i\text{-}C_4H_{10} \rightarrow NH_3 + C_4H_9$ (4) | | | | | | $(2.39 \times 10^{-23})T^{3.60}e^{-2239/T}$<br>$(3.35 \times 10^{-23})T^{3.57}e^{-1795/T}$(adj) | 300−520 K:[g] $(3.82 \times 10^{-13})e^{-4900/RT}$<br>470−973 K:[k] $(8.14 \times 10^{-13})e^{-5258/RT} + (1.46 \times 10^{-11})e^{-10397/RT}$ |
| $NH_2 + n\text{-}C_4H_{10} \rightarrow NH_3 + C_4H_9$ (5) | | | | | | 300−520 K:[g] $(1.16 \times 10^{-12})e^{-6100/RT}$ | |
| $NH_2 + C_6H_{12} \rightarrow NH_3 + C_6H_{11}$ (6) | | | | | | | 544−973 K:[j] $(4.48 \times 10^{-11})e^{-8915/RT}$ |

[a] Heat of reaction calculated at the G2M(rcc,MP2) level. [b] Experimental enthalpy of reaction at 298 K, from ref 19. [c] Classical barrier at the G2M(rcc,MP2) level. [d] Quantum mechanical barrier at the G2M(rcc,MP2) level. [e] Adjusted barrier height. [f] Eckart tunneling correction was used to compute the rate constants. The adjusted expressions are obtained from TST calculations with adjusted barrier height. [g] From ref 4. [h] From ref 5. [i] From ref 8. [j] From ref 6. [k] From ref 7.

## Calculation Methods

The energies of the reactants, products, and transition states for the reactions of $NH_2$ with saturated hydrocarbons were calculated using different versions of the G2M method.[13,14] This involved geometry optimization and vibrational frequency calculations at the density functional B3LYP/6-311G(d,p) level.[15] The G2M(RCC), G2M(RCC,MP2), G2M(rcc,MP2), and G2M(rcc,MP2*) calculational schemes used herein were described in detail earlier.[13,14] All of them were targeted to approximate the RCCSD(T)/6-311+G(3df,2p) energy through a series of RCCSD(T), MP4, and MP2 calculations with different basis sets. We used the GAUSSIAN 94[16] and MOLPRO 96[17] programs for the ab initio calculations. Optimized geometries of the transition states are presented in Figure 1.

For the thermal rate constant calculations, we employed TST with the Wigner and Eckart tunneling corrections.[18] The B3LYP/6-311G(d,p) molecular parameters of the reactants and transition states used for the rate computations are given in Table 2. Total energies for the optimized geometries of various species are summarized in Table 3.

## Results and Discussion

**$NH_2 + CH_4$.** The transition state for reaction 1, TS1, has a structure with a nearly linear N−H−C fragment and NH and CH distances of 1.26 and 1.33 Å, respectively. Both NH and CH bonds are elongated by about 22% as compared to the regular NH and CH bond lengths, respectively. Thus, the transition state is neither early nor late, which agrees with the fact that the $NH_2 + CH_4 \rightarrow NH_3 + CH_3$ reaction is nearly thermoneutral (exothermic by 2−3 kcal/mol). The lowest real vibrational frequency of TS2 is 49 $cm^{-1}$. This normal mode corresponds approximately to internal rotation around the C−N axis. Therefore, in the rate constant calculations we replaced this vibration by a one-dimensional internal rotation. The reduced moment of inertia shown in Table 2 was computed based on the geometry of TS1. As seen in Table 3, all G2M versions give the barrier height in the 14.9−15.4 kcal/mol range, close to the CCSD(T)/6-311++G(2d,p) result of Basch and Hoz.[11] The lowest value, 14.9 kcal/mol, found at G2M(rcc,MP2) was used for the rate constant computations.

Figure 2 shows the Arrhenius plot of the calculated and experimental rate constants for reaction 1. With the barrier of 14.9 kcal/mol and the Wigner tunneling correction, the theoretical rate constants significantly underestimate the low-temperature data of Demissy and Lesclaux,[4] agree reasonably well with the values of Hack et al.[5] in the 740−1030 K temperature range, and overestimate the shock tube high-temperature data of Hennig and Wagner.[8] The activation energies computed from the two-parameter fit of the theoretical rate constants, 13.9, 16.7, and 22.7 kcal/mol for the temperature ranges of 300−520, 740−1030, and 1740−2140 K, respectively, overestimate the corresponding experimental values of 10.5, 13.2, and 15.2 kcal/mol. If the reaction barrier is reduced by 1 kcal/mol to 13.9 kcal/mol, the agreement of the theoretical rate constant with the low-temperature experiment improves [$k_1$(theor) = (0.24−1.36)$k_1$(exp)] and is still fair for the 740−1030 K range [$k_1$(theor) = (2.1−3.4)$k_1$(exp)]. However, for the 1740−2140 K interval, the calculated rate constants are higher by 1 order of magnitude than the experimental data of Hennig and Wagner.[8] The computed activation energies for the three temperature intervals, 12.9, 15.6, and 21.7 kcal/mol, respectively, still overestimate the activation energies derived from experiment. Further reduction of the barrier height leads to an increasing disagreement of the theoretical rate constants with experiment in the medium-

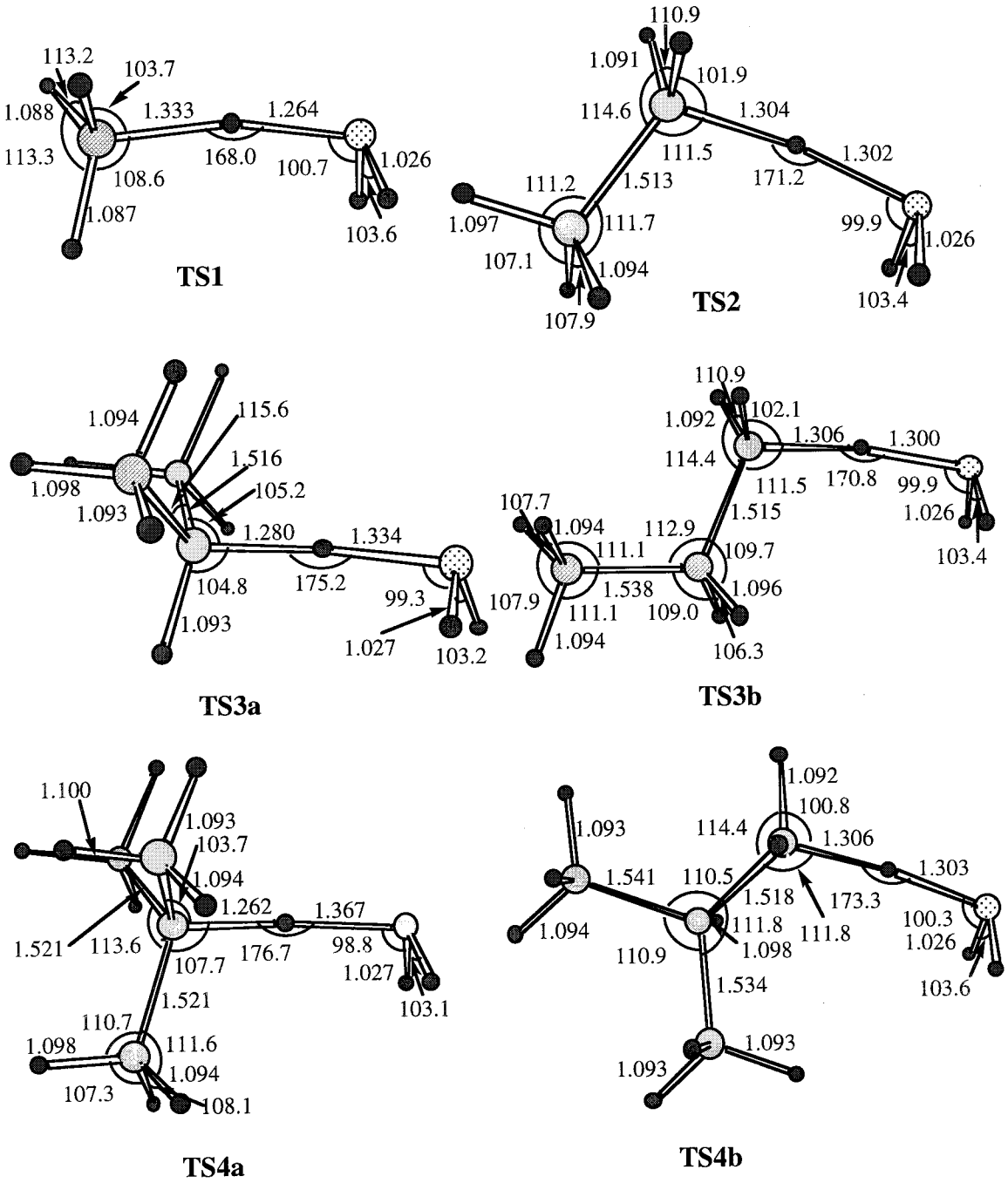


**Figure 1.** B3LYP/6-311G(d,p) optimized geometries of transition states for reactions 1−4. Bond lengths are given in angstroms and bond angles in degrees.

and high-temperature ranges. Thus, the calculations predict a stronger upward curvature for the Arrhenius plot of $k_1$ than that observed experimentally.

The use of the Eckart tunneling correction improves agreement of the calculated rate constant with experiment, especially in the low-temperature region. If the barrier is not adjusted (14.9 kcal/mol), theoretical $k_1$ constitutes 34−68% of $k_1$(exp) for 300−520 K. For higher temperatures, $k_1$(theor) = (1.1−2.1)$k_1$(exp) and (6.1−8.4)$k_1$(exp) in the 740−1030 and 1740−2140 K ranges, respectively. A small adjustment of the barrier height to 14.4 kcal/mol results in a very close agreement of the theoretical and experimental rate constants between 300 and 520 K, and the apparent activation energy from the two-parameter fit of $k_1$(theor) is 10.8 kcal/mol, only 0.3 kcal/mol higher than that experimentally found. At higher temperatures, tunneling is not significant, and $k_1$ values calculated with the Eckart and Wigner tunneling corrections are similar.

In this study, we use a three-parameter fit for the rate constants where they are expressed as $AT^b \exp(-E/T)$. This expression is a simple way to describe a non-Arrhenius behavior of the rate constants and to fit them in a broad temperature range. Besides, this form of expression is used widely in practical applications, for example, for kinetic modeling using the CHEMKIN program.[19] The three-parameter fit for 300−5000 K of the theoretical rate constant computed with the 14.4 kcal/mol barrier and Eckart tunneling correction resulted in the following expression for $k_1$:

$$k_1 = (5.12 \times 10^{-23})T^{3.59} \exp(-4{,}547/T)\ \mathrm{cm^3\ molecule^{-1}\ s^{-1}}$$

**TABLE 2: Molecular and Transition-State Parameters of the Reactants and Transition States of the $NH_2 + CH_4$, $NH_2 + C_2H_6$, $NH_2 + C_3H_8$, and $NH_2 + C_4H_{10}$ Reactions, Calculated at the B3LYP/6-311G(d,p) Level**

| species | i | ($10^{-40}$ g cm$^2$) $I_i$ | ($10^{-40}$ g cm$^2$) $I_{introt}$ | $\nu_j$ (cm$^{-1}$) | ZPE (kcal/mol) |
|---|---|---|---|---|---|
| $NH_2$ | A | 1.239 | | 1535, 3325, 3413 | 11.8 |
| | B | 2.169 | | | |
| | C | 3.408 | | | |
| $CH_4$ | A | 5.347 | | 1342, 1342, 1342, 1561, 1561, 3026 | 28.0 |
| | B | 5.347 | | 3131, 3131, 3131 | |
| | C | 5.347 | | | |
| TS1 | A | 8.919 | 2.142 | 1649i, 49,[a] 388, 401, 569, 786, 859, 1160, | 39.7 |
| | B | 95.97 | | 1367, 1425, 1441, 1502, 1576, 3054, 3179, | |
| | C | 97.00 | | 3183, 3386, 3476 | |
| $C_2H_6$ | A | 10.49 | | 310, 827, 829, 997, 1215, 1218, 1406, | |
| | B | 42.46 | | 1426, 1506, 1506, 1507, 1508, 3025, 3026, | |
| | C | 42.26 | | 3072, 3072, 3097, 3097 | |
| TS2 | A | 35.96 | 3.308 | 1611i, 34,[a] 155, 200, 422, 534, 742, 751, 881, 924, 1034, 1151, 1228, | 57.9 |
| | B | 169.8 | | 1390, 1412, 1467, 1477, 1495, 1497, 1562, 3003, 3052, 3062, | |
| | C | 190.6 | | 3080, 3130, 3378, 3468 | |
| $C_3H_8$ | A | 28.59 | | 230, 285, 369, 749, 842, 912, 936, 1059, 1177, 1210, | 64.7 |
| | B | 101.1 | | 1315, 1363, 1407, 1424, 1489, 1494, 1498, 1512, | |
| | C | 114.0 | | 1512, 3014, 3016, 3020, 3034, 3074, 3084, 3085, 3087 | |
| TS3a | A | 111.3 | 3.374 | 1479i, 43,[a] 121, 148, 189, 253, 355, 483, 656, 740, 874, 931, 945, 953, 1113, 1179, | 75.6 |
| | B | 202.3 | | 1206, 1352, 1356, 1401, 1416, 1468, 1482, 1490, 1496, 1501, 1558, | |
| | C | 283.5 | | 2996, 3000, 3051, 3058, 3063, 3087, 3093, 3374, 3465 | |
| TS3b | A | 41.29 | 3.397 | 1614i, 52,[a] 92, 124, 248, 319, 422, 586, 736, 742, 800, 901, 940, 995, 1064, 1135, | 75.9 |
| | B | 341.7 | | 1218, 1317, 1347, 1386, 1408, 1466, 1476, 1491, 1499, 1509, | |
| | C | 362.7 | | 1562, 3012, 3020, 3038, 3050, 3084, 3087, 3121, 3379, 3469 | |
| $C_4H_{10}$ | A | 109.0 | | 211, 257, 257, 363, 367, 435, 796, 923, 925, 956, 971, 971, 1191, 1191, 1209, | 82.2 |
| | B | 109.0 | | 1360, 1360, 1401, 1401, 1430, 1484, 1490, 1490, 1509, 1509, 1516, | |
| | C | 188.5 | | 2993, 3011, 3011, 3018, 3070, 3070, 3079, 3080, 3083, 3083 | |
| TS4a | A | 194.3 | 3.404 | 1518i, 39,[a] 111, 122, 194, 227, 235, 330, 363, 367, 527, 669, 778, 808, 952, 953, 972, | 94.0 |
| | B | 293.6 | | 1022, 1024, 1198, 1254, 1262, 1368, 1423, 1425, 1450, 1494, 1503, 1510, 1513, 1526, | |
| | C | 294.3 | | 1531, 1537, 1616, 3013, 3013, 3021, 3078, 3083, 3086, 3107, 3115, 3118, 3344, 3447 | |
| TS4b | A | 116.5 | 3.417 | 1702i, 72,[a] 83, 127, 232, 261, 314, 365, 400, 447, 582, 713, 823, 832, 939, 951, 971, | 94.4 |
| | B | 366.4 | | 983, 1050, 1165, 1201, 1226, 1357, 1380, 1399, 1425, 1443, 1483, 1518, 1520, 1530, | |
| | C | 441.3 | | 1533, 1539, 1622, 3011, 3036, 3041, 3072, 3100, 3106, 3112, 3114, 3146, 3361, 3465 | |

[a] In rate constant calculations, this frequency is replaced by a one-dimensional internal rotor with the reduced moment of inertia $I_{introt}$.

**TABLE 3: Calculated Energetics (kcal/mol, ZPE corrections are included) for the Reactions 1−4 at Various Levels of Theory: C−H Bond Strengths in Alkanes, Heats of Reactions ($\Delta E$), and Activation Barriers ($\Delta E^{\#}$)**

| reaction | B3LYP/ 6-311G** | CCSD(T)/ 6-31G** | CCSD(T)/ 6-311G** | G2M (RCC) | G2M (RCC,MP2) | G2M (rcc,MP2) | G2M (rcc,MP2*) |
|---|---|---|---|---|---|---|---|
| $NH_2 + CH_4 \rightarrow NH_3 + CH_3$ (1) | | | | | | | |
| C−H bond strength | 102.2 | 100.6 | 99.7 | 104.6 | 104.3 | 104.2 | 104.0 |
| $\Delta E$ | −0.3 | 1.8 | 0.2 | −1.7 | −2.1 | −2.3 | −2.1 |
| $\Delta E^{\#}$ | 10.2 | 18.5 | 16.0 | 15.2 | 15.1 | 14.9 | 15.4 |
| $NH_2 + C_2H_6 \rightarrow NH_3 + C_2H_5$ (2) | | | | | | | |
| C−H bond strength | 97.3 | 97.4 | 97.0 | 101.3 | 101.1 | 100.7 | 100.5 |
| $\Delta E$ | −5.2 | −1.3 | −2.5 | −5.0 | −5.3 | −5.7 | −5.6 |
| $\Delta E^{\#}$ | 7.7 | 15.7 | 13.7 | 12.7 | 12.7 | 12.2 | 12.7 |
| $NH_2 + C_3H_8 \rightarrow NH_3 + i\text{-}C_3H_7$ (3a) | | | | | | | |
| C−H bond strength | 92.4 | 94.7 | 94.3 | 98.5 | 98.4 | 98.3 | 98.1 |
| $\Delta E$ | −10.0 | −4.0 | −5.2 | −7.8 | −8.1 | −8.2 | −8.1 |
| $\Delta E^{\#}$ | 4.2 | 12.9 | 9.7 | | 8.6 | 8.4 | 8.6 |
| $NH_2 + C_3H_8 \rightarrow NH_3 + n\text{-}C_3H_7$ (3b) | | | | | | | |
| C−H bond strength | 96.9 | 98.1 | 97.4 | 101.8 | 101.5 | 101.4 | 101.2 |
| $\Delta E$ | −5.5 | −0.6 | −2.1 | −4.6 | −4.9 | −5.0 | −4.9 |
| $\Delta E^{\#}$ | 6.7 | 15.5 | 13.3 | | 11.3 | 11.1 | 11.6 |
| $NH_2 + i\text{-}C_4H_{11} \rightarrow NH_3 + t\text{-}C_4H_9$ (4a) | | | | | | | |
| C−H bond strength | 90.6 | 92.9 | 92.9 | | 96.9 | 96.8 | 96.7 |
| $\Delta E$ | −11.9 | −6.0 | −6.7 | | −9.7 | −9.8 | −9.7 |
| $\Delta E^{\#}$ | 4.5 | 11.7 | | | | 8.3 | 8.8 |
| $NH_2 + i\text{-}C_4H_{10} \rightarrow NH_3 + i\text{-}C_4H_9$ (4b) | | | | | | | |
| C−H bond strength | 97.9 | 98.4 | 97.6 | | 101.7 | 101.6 | 101.4 |
| $\Delta E$ | −4.6 | −0.5 | −2.0 | | −4.9 | −5.0 | −5.0 |
| $\Delta E^{\#}$ | 9.0 | 17.2 | | | | 12.4 | 12.9 |

This expression better reproduces the experimental data for low temperatures than the expression derived previously[12] that employed the Wigner tunneling correction and the barrier adjustment to 13.9 kcal/mol.

The Wigner tunneling correction is an approximation corresponding to an asymptotic form of the Eckart correction.[18] This approximation should be accurate for small barrier heights and widths, which apparently is not the case for the $NH_2 + CH_4$

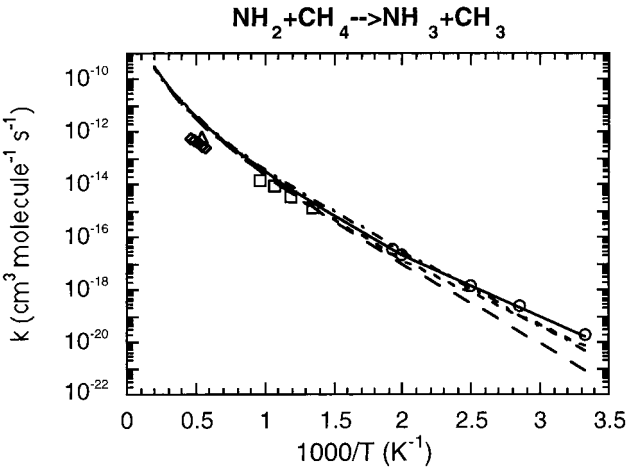


**Figure 2.** Arrhenius plot of the rate constant $k_1$ for the $NH_2 + CH_4$ reaction. Long-dashed and dashed-dotted curves show $k_1$ calculated with the Wigner tunneling correction with the barriers of 14.9 (G2M-(rcc,MP2)) and 13.9 (adjusted) kcal/mole, respectively. Short-dashed and solid curves show $k_1$ calculated with the Eckart tunneling correction with the barriers of 14.9 and 14.4 kcal/mol, respectively. Experimental rate constants are shown by open circles (ref 4), squares (ref 5), diamonds, and triangles (ref 8).

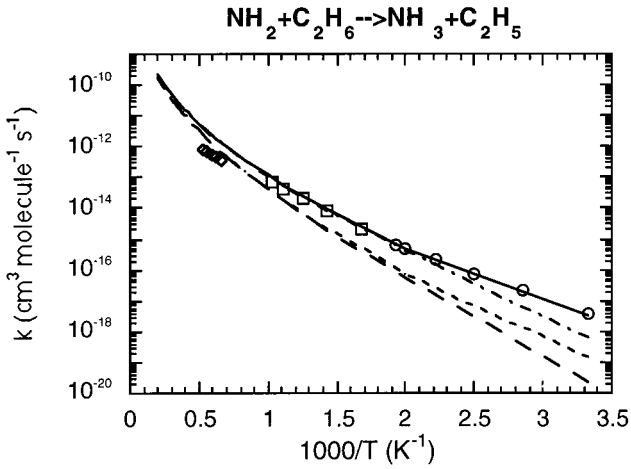


**Figure 3.** Arrhenius plot of the rate constant $k_2$ for the $NH_2 + C_2H_6$ reaction. Long-dashed and dashed-dotted curves show $k_2$ calculated with the Wigner tunneling correction with the barriers of 12.2 (G2M-(rcc,MP2)) and 10.2 (adjusted) kcal/mol, respectively. Short-dashed and solid curves show $k_2$ calculated with the Eckart tunneling correction with the barriers of 12.2 and 10.2 kcal/mol, respectively. Experimental rates are shown by open circles (ref 4), squares (ref 6), and diamonds (ref 8).

reaction. Several approaches exist to improve treatment of tunneling since the Eckart correction is valid only for a special barrier shape.[18] For instance, for systems in which the curvature of the reaction path is not too severe, the small-curvature tunneling (SCT) method[20,21] includes the effect of the reaction path curvature to induce the tunneling path to "cut the corner" and shorten the tunneling length. However, for the heavy−light−heavy mass combination present in the reactions of $NH_2$ with alkanes, the SCT method may not be suitable. This can be illustrated by two examples. Espinosa-Garcia and Corchado have studied[22] the tunneling effect in the $NH_3 + OH$ reaction and found that the rate at 300 K computed with SCT correction underestimates the experimental value by a factor of 16, while the Eckart tunneling correction gives the value only 1.8 times lower than that obtained in the experiment. On the other hand, a recent study of the $NH_2 + CH_4$ reaction by Yu et al.[23] shows that the rate constant at 300 K obtained with SCT correction overestimates the experimental rate by 7.7 times. In our calculations with the Eckart tunneling correction, the difference between the theoretical and experimental rate constants at 300 K is only 6%. Espinosa-Garcia and Corchado argue that for the heavy−light−heavy reactions a large-curvature tunneling (LCT) would be more appropriate. However, the LCT approach requires more information about the potential energy surface and can be too demanding computationally for the reactions, such as $NH_2 + C_3H_8$ or $NH_2 + C_4H_{10}$. Besides, the LCT method has only been applied in a few systems. The Eckart tunneling factor is overestimated at low temperatures because of the potential being much narrower in the "tail region" than the true adiabatic potential.[24,25] Therefore, according to Espinosa-Garcia and Corchado's results for $NH_3 + OH$, the simple Eckart model simulates the behavior of the more sophisticated LCT results. Later, this conclusion was confirmed by Truhlar and co-workers[26] at a more complete level, the microcanonical optimized multidimensional tunneling ($\mu$OMT) method, in which the transmission probability is taken as the maximum of two trial calculations, SCT and LCT. The $\mu$OMT rate constants agree better with the experimental results, but their difference from the rates obtained with the Eckart tunneling correction does not exceed ~80%. Hence, the accuracy of the Eckart approach should be reasonable, and because of its simplicity, we use this method in the present study for the reactions of $NH_2$ with alkanes.

Another question related to the accuracy of the present calculations concerns the use of variational TST (VIST) instead of conventional TST (CTST). For the reaction with a relatively high and distinct barrier, the variational effects are usually insignificant. For example, only a small rate constant decrease from CTST to VTST was found for the $NH_3 + OH$[26] and, especially, $C_2H_3 + H_2$[27] reactions with the barriers of 3.7 and 10.4 kcal/mol, respectively. The recent study of $NH_2 + CH_4$ by Yu et al.[23] demonstrated that the VTST rate constants deviate from the CTST ones by less than 5%. Thus, for the reactions of $NH_2$ with alkanes where the barriers are in the 8−15 kcal/mol range, the variational effects on the rate constant can be neglected.

**$NH_2 + C_2H_6$.** The $NH_2 + C_2H_6$ reaction (2) is calculated to have a barrier of 12.2−12.7 kcal/mol. The primary C−H bond in ethane, 101.3 kcal/mol at G2M(RCC) or 101.1 kcal/mol in experiment,[28] is weaker than that in methane, 104.8 kcal/mol.[28] As a result, reaction 2 is more exothermic than reaction 1 and the activation barrier for the hydrogen abstraction decreases by ~2.5 kcal/mol. The transition state TS2 has an earlier character than TS1; the forming N−H bond in the former is 0.04 Å longer than that in the latter, and the breaking C−H bond in TS2 is 0.03 Å shorter than that in TS2. The CHN angle increases from 168.0° in TS1 to 171.2° in TS2. Similar to TS1, the lowest real vibrational frequency in TS2 is very low, 34 $cm^{-1}$, and was replaced by internal rotation in computations of the rate constants.

Figure 3 shows the Arrhenius plot for the calculated thermal rate constants for reaction 2. First, we analyze the rates computed with the Wigner tunneling correction. If the G2M-(rcc,MP2) barrier height of 12.2 kcal/mol is taken for the rate constant calculations, theoretical values underestimate the experimental data in the 300−520 and 598−973 K temperature ranges and slightly overestimate the experimental measurements [$k_2$(theor) = (1.9−3.2)$k_2$(exp)] in the shock tube temperature range. The computed activation energies, 11.6, 13.7, and 19.0 kcal/mol for the temperature ranges of 300−520, 598−973, and

1500−1900 K, respectively, also overestimate those derived from experiment, 7.2, 10.6, and 11.5 kcal/mol. Therefore, we tried to adjust the barrier height, reducing it by 2.0 kcal/mol. Then, the agreement with experiment improves significantly. In the 300−520 K range, $k_2$(theor) equals to (0.19−0.93)$k_2$(exp); in the 598−973 K range, the difference between the experimental and calculated rate constants is less than 40%. In the high-temperature range, the deviation of theory from experiment increases, $k_2$(theor) = (3.7−5.5)$k_2$(exp). The computed activation energies are 9.6, 11.7, and 17.0 kcal/mol for the three temperature ranges, respectively. As for reaction 1, theoretical calculations for reaction 2 predict stronger curving for the Arrhenius plot when temperature is increasing, and differences between the calculated and experimental rate constants are largest for the shock tube region.

A much better agreement of theoretical $k_2$ with the low-temperature observations is found when we use the Eckart tunneling correction. With the barrier reduced to 10.2 kcal/mol, $k_2$(theor) = (0.75−1.18)$k_2$(exp) for 300−520 K, (1.12−1.41)-$k_2$(exp) for 598−973 K, and (3.7−5.6)$k_2$(exp) for 1500−1900 K. The activation energy computed in the 300−520 K temperature range is then 7.6 kcal/mol compared with 7.2 kcal/mol found experimentally. The three-parameter fit in the temperature range of 300−5000 K using theoretical rate constants calculated with the adjusted barrier and Eckart's tunneling gives the following expression for $k_2$:

$$k_2 = (7.54 \times 10^{-23}) T^{3.46} \exp(-2820/T) \text{ cm}^3 \text{ molecule}^{-1} \text{ s}^{-1}$$

**$NH_2$ + $C_3H_8$.** For the reaction of $NH_2$ with propane, H-atom abstraction from one of the primary as well as a secondary C−H bonds can occur. The secondary C−H bond (∼98.5 kcal/mol both in theory and in experiment[28]) is weaker than the primary one (101.8 kcal/mol at G2M(RCC) vs 100.4 kcal/mol in experiment[28]), and reaction 3a producing *i*-$C_3H_7$ is calculated to be 3.2 kcal/mol more exothermic than reaction 3b producing *n*-$C_3H_7$. Accordingly, the activation barrier for reaction 3a, 8.4 kcal/mol at the G2M(rcc,MP2) level, is 2.7 kcal/mol lower than that for reaction 3b, 11.1 kcal/mol. The structure of transition states TS3a and TS3b reflects the reaction energetics. TS3a is an earlier transition state as compared to TS3b, TS2, or TS1. It has a shorter breaking C−H bond of 1.28 Å and a longer forming N−H bond of 1.33 Å. The linearity of the CHN fragment increases and the corresponding angle is 175.2°. On the other hand, the geometry of TS3b is very similar to that of TS2, except a hydrogen atom is replaced by a methyl group. The activation barrier for (3b) is about 1 kcal/mol lower than the barrier for (2); however, this difference is within the accuracy of our calculations.

The total rate constant for the reaction 3, $NH_2$ + $C_3H_8$, as measured in the experiment, is the sum of the individual rate constants for reactions 3a and 3b. Figure 4a shows the Arrhenius plots for the total rate constant $k_3$ in comparison with the experiment. As seen from the plots, the rates computed with the Eckart tunneling correction match better the experimental measurements than those obtained with the Wigner correction. Therefore, below we discuss only $k_3$ with Eckart's tunneling. If we use for the TST computations the G2M(rcc,MP2) barriers, 8.4 and 11.1 kcal/mol for reactions 3a and 3b, respectively, the theoretical values of $k_3$ agree with experiment reasonably well. In the 300−520 K temperature range, $k_3$(theor) equals to (0.41−0.77)$k_3$(exp). The accord is best in the 550−1073 K range: $k_3$-(theor) = (0.92−1.69)$k_3$(exp). Theoretical rate constants for the high temperature 1500−1900 K range overestimate the experimental values; $k_3$(theor) is a factor of 2.6−4.1 higher than $k_3$-

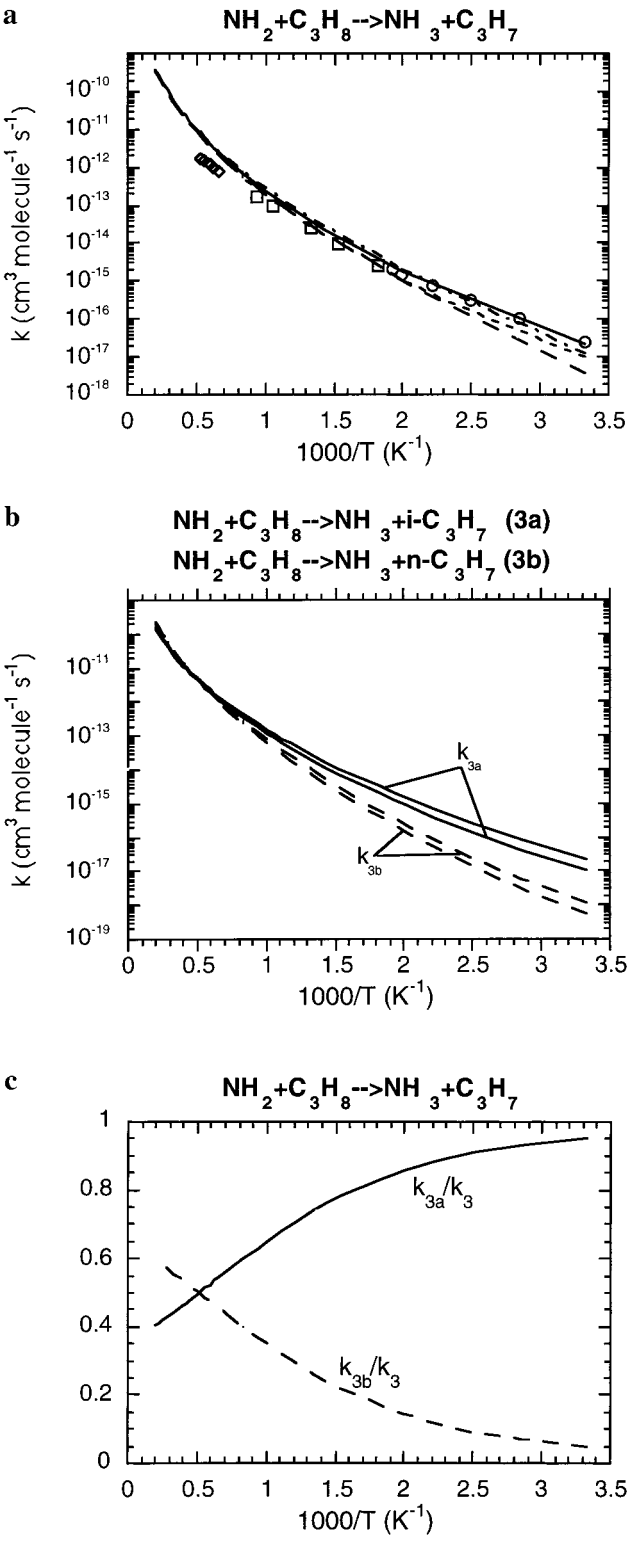


**Figure 4.** (a) Arrhenius plot of the rate constant $k_3$ for the $NH_2$ + $C_3H_8$ reaction. Long-dashed and dashed-dotted curves show $k_3$ calculated with the Wigner tunneling correction with the G2M(rcc,MP2) (8.4 kcal/mol for the (3a) channel and 11.1 kcal/mol for (3b)) and the adjusted (7.7 kcal/mol for (3a) and 10.4 kcal/mol for (3b)) barriers, respectively. Short-dashed and solid curves show $k_3$ calculated with the Eckart tunneling correction with the 8.4/11.1 and 7.9/10.6 kcal/mol barriers, respectively. Experimental rates are shown by open circles (ref 4), squares (ref 7), and diamonds (ref 8). (b) Arrhenius plot of the calculated individual rate constants $k_{3a}$ (solid curves) and $k_{3b}$ (dashed curves). (c) Calculated $k_{3a}/k_3$ and $k_{3b}/k_3$ branching ratios as function of temperature.

(exp). The computed activation energies for the three temperature ranges are 7.0, 10.8, and 17.1 kcal/mol, respectively, vs 6.2, 9.3, and 10.7 kcal/mol derived from experiment. If the barriers for both reactions 3a and 3b are reduced by 0.5 kcal/mol to 7.9 and 10.6 kcal/mol, respectively, the deviations of theory from the experiment are very small for the low-temperature range [$k_3$(theor) = (0.94−1.25)$k_3$(exp)] and slightly increase for the middle- [$k_3$(theor) = (1.4−2.1)$k_3$(exp)] and high- [$k_3$(theor) = (3.0−4.7)$k_3$(exp)] temperature ranges. The computed activation energies, 6.6, 10.3, and 16.7 kcal/mol for the 300−520, 550−1073, and 1500−1900 K temperature ranges, respectively, reproduce better the experimental values, especially for low temperatures. As for reactions 1 and 2, the calculations for reaction 3 tend to overestimate the experimental activation energies in the high-temperature region and to predict a stronger curvature in the Arrhenius plot at higher temperatures. Whereas the absolute values of the theoretical and experimental rate constants $k_3$ agree fairly well, their disagreement is significant in the shock tube region. The total theoretical rate constant $k_3$ calculated with the adjusted barrier heights is fitted in the temperature range of 300−5000 K by the following three-parameter expression:

$$k_3 = (3.49 \times 10^{-23}) T^{3.60} \exp(-2249/T)\ \mathrm{cm^3\ molecule^{-1}\ s^{-1}}$$

Figure 4b exhibits the individual rate constants $k_{3a}$ and $k_{3b}$, and Figure 4c shows the calculated temperature dependence of the $k_{3a}/k_3$ and $k_{3b}/k_3$ branching ratios. Because of the lower activation barrier, reaction 3a is faster than reaction 3b at temperatures below 2000 K. In the low temperature 300−500 K region, the rate constant for the abstraction of a secondary C−H bond in $C_3H_8$ constitutes 85−95% of the total rate constant. The contribution of $k_{3a}$ into $k_3$ decreases to 65 and 50% when temperature increasing to 1000 and 2000 K, respectively. Reaction 3b becomes dominant at the temperatures higher than 2000 K.

**$NH_2$ + *i*-$C_4H_{10}$.** The reaction of $NH_2$ with isobutane also can proceed by two different channels: the abstraction of a hydrogen atom from a tertiary and a primary C−H bond. The tertiary C−H bond in *i*-$C_4H_{10}$ is calculated to be 4.8 kcal/mol weaker than the primary one, which results in the higher exothermicity of the 4a channel as compared to (4b). The agreement between theory and experiment for the tertiary C−H bond strength is close again, 96.9 kcal/mol at the G2M-(RCC,MP2) level vs the experimental value of 96.4 kcal/mol.[28] The G2M(rcc,MP2) barriers are found to be 8.3 and 12.4 kcal/mol for (4a) and (4b), respectively. Transition state TS4a is the earliest TS among all transition states for the hydrogen atom abstraction from C−H bonds in the alkanes considered in the present study. It has the shortest breaking C−H bond, 1.26 Å, and the longest forming N−H bond, 1.37 Å. The linearity of the CHN fragment is also maximal, with the CHN angle of 176.7°. The structure of TS4b is again very similar to those of TS2 and TS3b, indicating that the geometry of a TS for the H abstraction from a primary C−H bond is not sensitive to the size of the carbon chain in alkanes.

The Arrhenius plot for the total rate constant for the $NH_2$ + *i*-$C_4H_{10}$ reaction, $k_4 = k_{4a} + k_{4b}$, is shown in Figure 5a, while individual rate constants $k_{4a}$ and $k_{4b}$ are presented in Figure 5b. Experimental data for $k_4$ are available only for two temperature ranges, 300−520 and 470−973 K. Using the calculated G2M-(rcc,MP2) barriers of 8.3 and 12.4 kcal/mol for (4a) and (4b), respectively, and the Eckart tunneling correction, we obtained $k_4$, which underestimates the experimental data in both temperature regions. For instance, in the 300−520 K range, $k_4$-

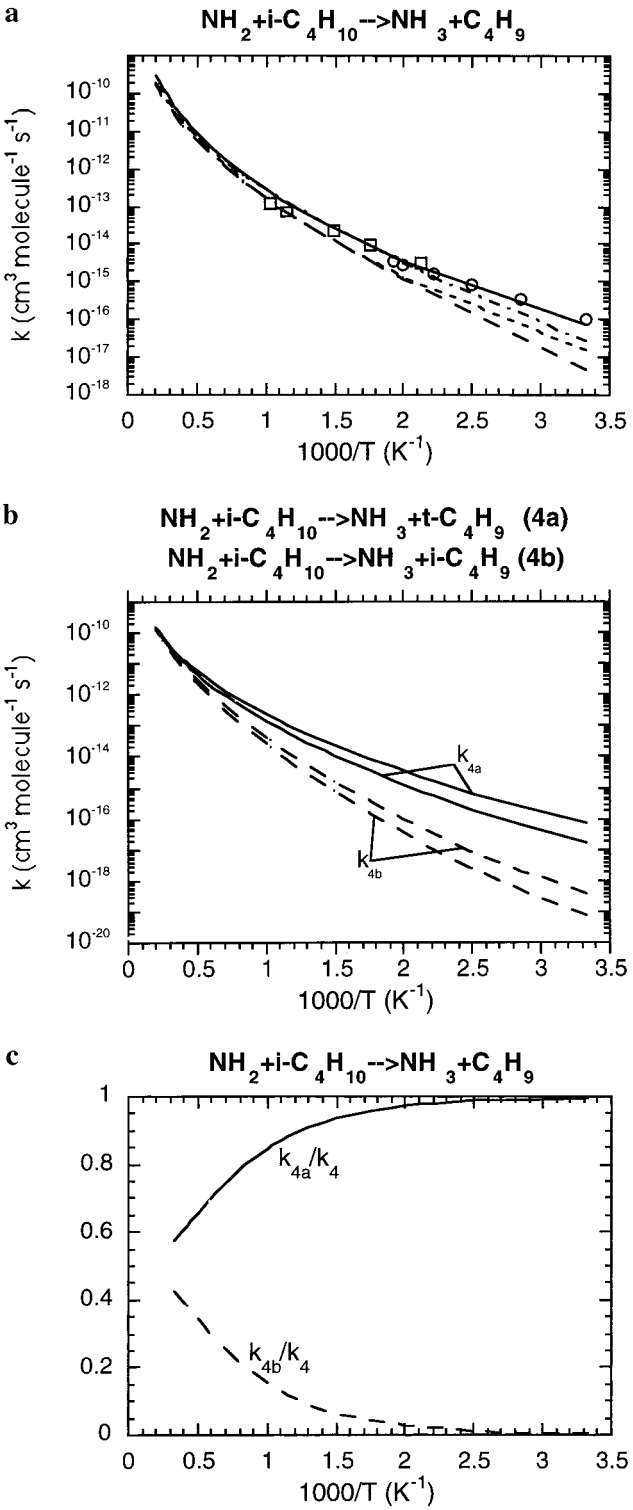


**Figure 5.** (a) Arrhenius plot of the rate constant $k_4$ for the $NH_2$ + *i*-$C_4H_{10}$ reaction. Long-dashed and dashed-dotted curves show $k_4$ calculated with the Wigner tunneling correction with the G2M(rcc,MP2) (8.3 kcal/mol for the (4a) channel and 12.4 kcal/mol for (4b)) and the adjusted (7.3 kcal/mol for (4a) and 11.4 kcal/mol for (4b)) barriers, respectively. Short-dashed and solid curves show $k_4$ calculated with the Eckart tunneling correction with the 8.3/12.4 and 7.3/11.4 kcal/mol barriers, respectively. Experimental rates are shown by open circles (ref 4) and squares (ref 6). (b) Arrhenius plot of the calculated individual rate constants $k_{4a}$ (solid curves) and $k_{4b}$ (dashed curves). (c) Calculated $k_{4a}/k_4$ and $k_{4b}/k_4$ branching ratios as function of temperature.

(theor) is 15−54% of $k_4$(exp) and in the 470−973 K range, $k_4$ = (0.25−1.19)$k_4$(exp). The computed activation energies, 6.7

and 9.4 kcal/mol for the two temperature ranges, respectively, are higher than the experimental values of 4.9 and 5.3 kcal/mol. Reduction of the barriers by 1 kcal/mol each improves the agreement with experiment. In this case, $k_4$(theor) is (0.72−1.41)$k_4$(exp) and (0.7−2.0)$k_4$(exp) in the 300−520 and 470−973 K temperature ranges, respectively, and the computed activation energy in the low-temperature region decreases to 5.8 kcal/mol. The three-parameter fit for $k_4$ obtained with the adjusted activation barriers gave the following expression for 300 K ≤ $T$ ≤ 5000 K:

$$k_4 = (3.35 \times 10^{-23}) T^{3.57} \exp(-1795/T) \text{ cm}^3 \text{ molecule}^{-1} \text{ s}^{-1}$$

Channel (4a) dominates reaction 4 through the 300−3000 K temperature range. As shown in Figure 5c, the $k_{4a}/k_4$ ratio exceeds 85% at temperatures below 1000 K but decreases to 66 and 57% at 2000 and 3000 K, respectively.

## Concluding Remarks

For all the reactions of $NH_2$ with alkanes considered herein, we found a fairly good agreement of the theoretical rate constants with experiment if one tolerates the adjustment of the computed barrier heights by 0.5−2 kcal/mol, within the accuracy of the G2M method. Different schemes of the G2M approach give similar (within 1 kcal/mol) values for the reaction heats and activation barriers. Therefore, the cheapest versions of the method G2M(rcc,MP2) and G2M(rcc,MP2*) can be applied to larger systems without significant loss of the accuracy. The B3LYP method tends to underestimate reaction barriers, and CCSD(T) with moderate basis sets overestimates them. Both B3LYP and CCSD(T) calculations underestimate the strength of C−H bonds by 3−4 kcal/mol. G2M calculations should give the results close to those of the CCSD(T) calculations with large basis sets. Similar trends were shown earlier for the reactions of $NH_2$ with $H_2$, $H_2O$, and $NH_3$.[12]

In general, theoretical rate constants computed with the Wigner tunneling correction underestimate experimental values in the low-temperature range, and lowering the activation barriers does not entirely upset this deviation. A very close agreement for the low temperatures is reached by using the more accurate Eckart tunneling correction. The calculated activation energies somewhat overestimate the values derived from experimental measurements for 500−1000 K and, especially, for the shock tube temperature range (1500−2100 K). Absolute values of theoretical rate constants in this region are several times higher than the experimental rates. Further studies are required in order to understand the origin of this deviation.

The calculated activation barrier for the $NH_2 + CH_4$ reaction, 15.2 kcal/mol, is higher than that for the $NH_2 + H_2$ reaction, 13.7 kcal/mol at the same G2M(RCC) level of theory.[12] The abstraction of a hydrogen atom from a primary C−H bond in $C_2H_6$, $C_3H_8$, and $i$-$C_4H_{10}$ requires overcoming a barrier of 11−12 kcal/mol. The barrier height decreases to 8.4 and 8.3 kcal/mol for the abstraction from a secondary C−H bond in $C_3H_8$ and a tertiary C−H bond in $i$-$C_4H_{10}$, respectively, in line with the weakening strength of the C−H bond and the increase of the reaction exothermicity.

Table 4 illustrates relative rate constants of reactions 2−4 with respect to $NH_2 + CH_4$ (1). The H-abstraction from the tertiary C−H bond should be faster than H-abstraction the other reactions at $T$ ≤ 2000 K. The secondary H-abstraction is the second fastest reaction at temperatures below 1600 K, but at $T$ ≥ 2000 K, it becomes slightly slower than reactions 2 and 3b. The rate of the primary H-abstraction decreases with the increase of the alkane size, from ethane to propane and to isobutane. The activation barrier does not change significantly, but the preexponetial factor fitted in the 300−520 K range decreases from $9.4 \times 10^{-13}$ cm$^3$ molecule$^{-1}$ s$^{-1}$ for (2) to $8.3 \times 10^{-13}$ for (3b) and $3.6 \times 10^{-13}$ for (4b). At temperatures higher than 3000 K reactions 2−4 are slower than $NH_2 + CH_4$. This result is attributed to the higher activation energy for reaction 1; $k_1$ grows faster with temperature than $k_2$−$k_4$ and overtakes all individual rates $k_2$, $k_{3a}$, $k_{3b}$, $k_{4a}$, and $k_{4b}$ at 3000 K.

**TABLE 4: Calculated Relative Rate Constants for Reactions 2−4 with Respect to the Rate $k_1$ of the $NH_2 + CH_4$ Reaction at Various Temperatures**

| $T$, K | $C_2H_6$ $k_2$ | $C_3H_8$ p-C−H, $k_{3b}$ | $C_4H_{10}$ p-C−H, $k_{4b}$ | $C_3H_8$ s-C−H, $k_{3a}$ | $C_4H_{10}$ t-C−H, $k_{4a}$ |
|---|---|---|---|---|---|
| 300 | 199.2 | 66.0 | 20.8 | 1257 | 4223 |
| 500 | 23.5 | 11.8 | 4.43 | 71.4 | 159.7 |
| 1000 | 3.55 | 2.65 | 1.36 | 4.93 | 7.52 |
| 1400 | 2.05 | 1.72 | 1.12 | 2.23 | 2.96 |
| 1600 | 1.73 | 1.50 | .98 | 1.73 | 2.20 |
| 2000 | 1.36 | 1.24 | 0.76 | 1.22 | 1.45 |
| 2500 | 1.13 | 1.06 | 0.67 | 0.92 | 1.03 |
| 3000 | 0.99 | 0.95 | 0.61 | 0.76 | 0.82 |

The rate constants for the hydrogen abstraction by $NH_2$ from primary, secondary, and tertiary C−H bonds discussed in this study can serve as models for the reactions of the amino radical with other saturated hydrocarbons. For example, the rate constant measured for the $NH_2 + n$-$C_4H_{10}$ reaction[4] is close to that for $NH_2 + C_3H_8$. As in $C_3H_8$, the abstraction of an H atom in $n$-$C_4H_{10}$ can take place from a primary and a secondary C−H bond and this explains the observed similarity in the rate constants. The rate constant reported for the $NH_2 + C_6H_{12}$ reaction[6] has a similar exponential factor as that for $NH_2 + C_3H_8$ because of the fact that all C−H bonds in cyclohexane are secondary.

**Acknowledgment.** We are grateful to the US Department of Energy, Office of Basic Energy Sciences, for the support of this work under Grant No. DE-FG02-97ER14784. We are also thankful for the Cherry L. Emerson Center for Scientific Computation for the use of various programs and the computing facility.

## References and Notes

(1) Strobel, D. F. *Int. Rev. Phys. Chem.* **1983**, *3*, 145.
(2) Lyon, R. K. *Int. J. Chem. Kinet.* **1976**, *8*, 318; U.S. patent 3,900,554.
(3) Perry, R. A.; Siebers, D. L. *Nature* **1986**, *324*, 657.
(4) Demissy, M.; Lesclaux, R. *J. Am. Chem. Soc.* **1980**, *102*, 2897.
(5) Hack, W.; Kurzke, H.; Rouveirolles, P.; Wagner, H. Gg. In *Twenty-First Symposium (International) on Combustion*; The Combustion Institute: Pittsburgh, PA, 1986; p 905.
(6) Ehbrecht, J.; Hack, W.; Rouveirolles, P.; Wagner, H. Gg. *Ber. Bunsen-Ges. Phys. Chem.* **1987**, *91*, 700.
(7) Hack, W.; Kurzke, H.; Rouveirolles, P.; Wagner, H. Gg. *Ber. Bunsen-Ges. Phys. Chem.* **1986**, *90*, 1210.
(8) Hennig, G.; Wagner, H. Gg. *Ber. Bunsen-Ges. Phys. Chem.* **1995**, *99*, 863.
(9) Leroy, G.; Sana, M.; Tinant, A. *Can. J. Chem.* **1985**, *63*, 1447.
(10) Sana, M.; Leroy, G.; Villaveces, J. L. *Theor. Chim. Acta* **1984**, *65*, 109.
(11) Basch, H.; Hoz, S. *J. Phys. Chem. A* **1997**, *101*, 4416.
(12) Mebel, A. M.; Moskaleva, L. V.; Lin, M. C. *J. Mol. Struct. (THEOCHEM)*, in press.
(13) Mebel, A. M.; Morokuma, K.; Lin, M. C. *J. Chem. Phys.* **1995**, *103*, 7414.
(14) Liu, R.; Morokuma, K.; Mebel, A. M.; Lin, M. C. *J. Phys. Chem.* **1996**, *100*, 9314.
(15) (a) Becke, A. D. *J. Chem. Phys.* **1993**, *98*, 5648. (b) *J. Chem. Phys.* **1992**, *96*, 2155. (c) *J. Chem. Phys.* **1992**, *97*, 9173. (d) Lee, C.; Yang, W.; Parr, R. G. *Phys. Rev.* **1988**, *B 37*, 785.
(16) Frisch, M. J.; Trucks, G. W.; Schlegel, H. B.; Gill, P. M. W.; Johnson, B. G.; Robb, M. A.; Cheeseman, J. R.; Keith, T.; Petersson, G.

A.; Montgomery, J. A.; Raghavachari, K.; Al-Laham, M. A.; Zakrzewski, V. G.; Ortiz, J. V.; Foresman, J. B.; Cioslowski, J.; Stefanov, B. B.; Nanayakkara, A.; Challacombe, M.; Peng, C. Y.; Ayala, P. Y.; Chen, W.; Wong, M. W.; Andres, J. L.; Replogle, E. S.; Gomperts, R.; Martin, R. L.; Fox, D. J.; Binkley, J. S.; Defrees, D. J.; Baker, J.; Stewart, J. P.; Head-Gordon, M.; Gonzalez, C.; Pople, J. A. GAUSSIAN 94, Revision D.4; Gaussian, Inc.: Pittsburgh, PA, 1995.

(17) MOLPRO is a package of ab initio programs written by H.-J. Werner and P. J. Knowles, with contributions from J. Almlöf, R. D. Amos, M. J. O. Deegan, S. T. Elbert, C. Hampel, W. Meyer, K. Peterson, R. Pitzer, A. J. Stone, P. R. Taylor, and R. Lindh.

(18) Steinfeld, J. I.; Francisco, J. S.; Hase, W. L. In *Chemical Kinetics and Dynamics*; Prentice Hall: Englewood Cliffs, NJ, 1989.

(19) Kee, R. J.; Rupley, F. M.; Miller, J. A. Sandia Laboratories Report, SAND89−8009B, 1993.

(20) Skodje, R. T.; Truhlar, D. G.; Garrett, B. C. *J. Chem. Phys.* **1982**, *77*, 5955.

(21) Skodje, R. T.; Truhlar, D. G.; Garrett, B. C. *J. Phys. Chem.* **1981**, *85*, 3019.

(22) Espinosa-Garcia, J.; Corchado, J. C. *J. Chem. Phys.* **1994**, *101*, 8700.

(23) Yu, Y.-X.; Li S.-M.; Xu, Z.-F.; Li, Z.-S.; Sun, C.-C. *Chem. Phys. Lett.* **1998**, *296*, 131.

(24) (a) Garrett, B. C.; Koszykowski, M. L.; Melius, C. F.; Page, M. *J. Phys. Chem.* **1990**, *94*, 7096. (b) Isaacson, A. D.; Wang, L.; Scheiner, S. *J. Phys. Chem.* **1993**, *97*, 1765.

(25) Chandra, A. K.; Padma Malar, E. J.; Gapta, D. S. *Int. J. Quantum Chem.* **1992**, *41*, 371.

(26) Corchado, J. C.; Espinosa-Garcia, J.; Hu, W.-P.; Rossi, I.; Truhlar, D. G. *J. Phys. Chem.* **1995**, *99*, 687.

(27) Mebel, A. M.; Morokuma, K.; Lin, M. C. *J. Chem. Phys.* **1995**, *103*, 3440.

(28) *CRC Handbook of Chemistry and Physics*, 74th ed.; Lide, D. R., Ed.; Chemical Rubber: Boca Raton, FL, 1993.